PAPER *Special Section on Nonlinear Theory and its Applications*

Stability Boundaries Analysis of Electric Power System with DC Transmission Based on Differential-Algebraic Equation System*

Yoshihiko SUSUKI[†a)], ***Student Member***, **Takashi HIKIHARA**[†b)], ***Member***, ***and*** **Hsiao-Dong CHIANG**[††c)], ***Nonmember***

SUMMARY This paper discusses stability boundaries in an electric power system with dc transmission based on a differential-algebraic equation (DAE) system. The DAE system is derived to analyze transient stability of the ac/dc power system: the differential equation represents the dynamics of the generator and the dc transmission, and the algebraic equation the active and reactive power relationship between the ac system and the dc transmission. In this paper complete characterization of stability boundaries of stable equilibrium points in the DAE system is derived based on an energy function for the associated singularly perturbed (SP) system. The obtained result completely describes global structures of the stability boundaries in solution space of the DAE system. In addition the characterization is confirmed via several numerical results with a stability boundary.

key words: *power system, dc transmission, stability boundary, differential-algebraic equation, energy function*

1. Introduction

This paper is concerned with transient stability problem of electric power systems with dc transmissions. Recently dc transmissions have been widely applied to conventional electric power systems [1]–[4]. Transient stability of ac/dc power systems is mainly analyzed using numerical simulations: readers can refer to [1], [2]. On the other hand, in [1], [5], [6] analytical studies on the transient stability are performed based on energy function method and dynamical system theory. The obtained results in [1], [5], [6], however, do not sufficiently include the operation of power conversion apparatuses in dc transmissions and the power relationship between ac and dc transmissions. In terms of synthesis of stabilization controllers via dc transmissions [1], [2], [4] it is inevitable to clarify the transient stability of the ac/dc systems with taking the operation and the power relation into account. Unfortunately, the transient stability has not been completely clarified from analytical points of view.

A differential-algebraic equation (DAE) system is proposed for transient stability analysis of an electric power system with dc transmission [7]. The DAE system is described by a coupled system of differential and algebraic equations: the differential equation represents the dynamics of the generator and dc transmission, while the algebraic equation describes the active and reactive power relation between the ac system and dc transmission**. The DAE system keeps the structural characteristics of the power conversion and control setup in the dc transmission, and explicitly describes the power relation between the ac system and dc transmission.

The present paper discusses stability boundaries in the ac/dc power system based on the DAE system. The *stability boundaries* imply basin boundaries of stable equilibrium points (EPs) which correspond to post-fault steady states of the ac/dc system, and essentially govern its transient stability. In [7], [9] a stability boundary is numerically analyzed in the ac/dc system based on the DAE system. This paper theoretically characterizes stability boundaries of the DAE system. To do this we strongly rely on some fundamental results reported in [10], [11]. In particular we analyze the stability boundaries via an energy function for the associated singularly perturbed (SP) system. The analysis completely characterizes global structures of the stability boundaries in solution space of the DAE system. In addition we examine the obtained characterization and the existence of energy function via several numerical results with a stability boundary which have been partially reported in [7], [9].

This paper is organized as follows. In Sect. 2 we introduce an electric power system with dc transmission and derives a DAE system. Section 3 summarizes fundamental concepts of the theory of differential-algebraic equation systems. Section 4 provides with us characterization of stability boundaries in the DAE system based on an energy function. In Sect. 5 we discuss the obtained characterization via some numerical results with a stability boundary. Section 6 concludes this paper with summary and discussion of our main results.

2. System Configuration and Derivation of Differential-Algebraic Equation System

This section introduces a system configuration of an electric

Manuscript received January 5, 2004.
Manuscript revised May 27, 2004.
Final manuscript received May 27, 2004.

†The authors are with the Department of Electrical Engineering, Kyoto University, Kyoto-shi, 615-8510 Japan.
††The author is with the School of Electrical and Computer Engineering at Cornell University, Ithaca, NY 14853, USA.
a) E-mail: susuki@dove.kuee.kyoto-u.ac.jp
b) E-mail: hikihara@kuee.kyoto-u.ac.jp
c) E-mail: chiang@ece.cornell.edu

*This research is supported in part by the Ministry of Education, Culture, Sports, Sciences and Technology in Japan, The 21st Century COE Program, No. 14213201, and Grant-in-Aid for Scientific Research (C) No. 14550264, 2003 and Exploratory Research, No. 16656089, 2004.

**Similar DAE systems are also derived for voltage and transient stability analysis of general ac/dc power systems [1], [8].

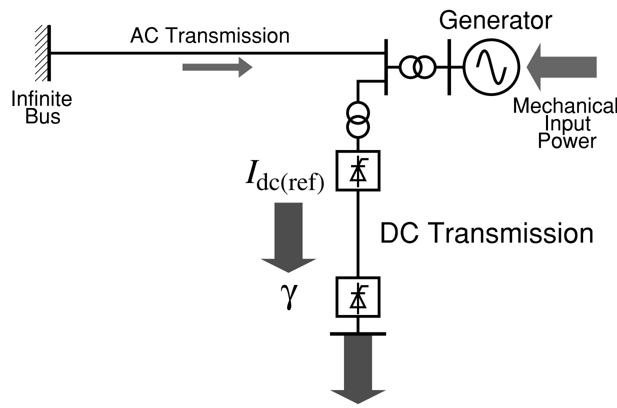

Fig. 1 System configuration of electric power system with dc transmission. The arrows denote the positive direction of active power flow.

power system with dc transmission, which we analyze in this paper, and derives a DAE system for transient stability analysis of the ac/dc power system [7]. Figure 1 shows the system configuration of the ac/dc power system. The ac/dc system is fixed based on the practical system [3], [4]. In the following discussion variables and parameters are normalized with the well-known per unit system.

First the dynamics of the generator is modeled based on Park's theory:

$$\begin{cases} \dfrac{T'_{d0}}{L_d - L'_d}\dot{v}'_q = \dfrac{V_0}{L_d - L'_d} + \dfrac{v_\mathrm{r}}{L'_d}\cos\delta_\mathrm{r} \\ \qquad\qquad - \dfrac{L_d}{L'_d(L_d - L'_d)}v'_q, \\ \dot{\delta} = \omega, \\ 2H\dot{\omega} = -D\omega + p_\mathrm{m} - p_\mathrm{g}, \end{cases} \tag{1}$$

where $\dot{v}'_q$ denotes the differentiation of v'_q by the normalized time t, v'_q the voltage source behind transient reactance, δ the rotor position with respect to the synchronously reference axis and ω the rotor speed difference relative to the system angular frequency. v_r and δ_r are defined for the bus voltage of the generator as follows:

$$e_d \triangleq v_\mathrm{r}\sin\delta_\mathrm{r}, \quad e_q \triangleq v_\mathrm{r}\cos\delta_\mathrm{r}, \tag{2}$$

where e_d and e_q represent the d-axis and q-axis terminal voltages of the generator. In (1) the parameters T'_{d0}, L_d, L'_d, H and D stand for the characteristics of the generator, and V_0 is related to the input voltage to the exciter. p_m represents the mechanical input power to the generator and p_g the active output power from the generator:

$$p_\mathrm{g} \triangleq \frac{v'_q v_\mathrm{r}}{L'_d}\sin\delta_\mathrm{r} + \frac{v_\mathrm{r}^2}{2}\frac{L'_d - L_q}{L'_d L_q}\sin 2\delta_\mathrm{r}. \tag{3}$$

(1) is derived under the assumption that sub-transient behavior in the generator is negligible. The effect of the control systems, which are AVR, PSS and so on, in the generator is also excluded to reveal native dynamics and stability of the ac/dc system.

Second the operation of the ac-dc converters is represented via the averaged model [1], [2]. It is here supposed that the ac-dc converters ideally operate under normal conditions and the harmonic components are completely filtered. The firing angle α of the rectifier is controlled according to

$$\alpha = G_\alpha(I_{\mathrm{dc(ref)}} - I_\mathrm{dc}), \tag{4}$$

where I_dc denotes the dc current, $I_{\mathrm{dc(ref)}}$ the reference current and G_α the gain coefficient of the rectifier controller. On the other hand, the inverter is controlled with keeping the margin angle γ constant [1], [2]. The averaged output dc voltage of the rectifier $V_{\mathrm{dc(r)}}$ and the averaged input one to the inverter $V_{\mathrm{dc(i)}}$ can be approximately given as follows:

$$\begin{cases} V_{\mathrm{dc(r)}} \approx K_V v_\mathrm{r}\cos\alpha - \dfrac{3}{\pi}X_\mathrm{c}I_\mathrm{dc}, \\ V_{\mathrm{dc(i)}} \approx K_V V_\mathrm{i}\cos\gamma - \dfrac{3}{\pi}X_\mathrm{c}I_\mathrm{dc}, \end{cases} \tag{5}$$

where K_V stands for the coupling coefficient between the ac bus and dc voltage, V_i the ac bus voltage at the inverter side and X_c the commutating reactance of the rectifier or inverter. The dynamics of the dc transmission is hence represented by

$$L_\mathrm{dc}\dot{I}_\mathrm{dc} = -R_\mathrm{dc}I_\mathrm{dc} + V_{\mathrm{dc(r)}} - V_{\mathrm{dc(i)}}, \tag{6}$$

where L_dc and R_dc denote the inductance and resistance in the dc transmission line, respectively.

Third the coupling relation between the ac system and dc transmission is modeled based on the active and reactive power relation. The relationship is given by

$$\begin{cases} 0 = p_\mathrm{g} + p_\mathrm{i} - K_I v_\mathrm{r} I_\mathrm{dc}\cos\varphi_\mathrm{r}, \\ 0 = q_\mathrm{g} + q_\mathrm{i} - K_I v_\mathrm{r} I_\mathrm{dc}\sin\varphi_\mathrm{r}, \\ 0 = K_I v_\mathrm{r} I_\mathrm{dc}\cos\varphi_\mathrm{r} - V_{\mathrm{dc(r)}}I_\mathrm{dc}, \end{cases} \tag{7}$$

where p_i denotes the active power which flows from the infinite bus, q_g the reactive power related to the generator and q_i the one related to the infinite bus. These power terms are represented by

$$\begin{cases} p_\mathrm{i} \triangleq \dfrac{v_\mathrm{r}V_\infty}{L_\infty}\sin(\delta_\mathrm{r} - \delta), \\ q_\mathrm{g} \triangleq \dfrac{v'_q v_\mathrm{r}}{L'_d}\cos\delta_\mathrm{r} - \dfrac{v_\mathrm{r}^2}{2}\dfrac{L'_d + L_q}{L'_d L_q} \\ \qquad + \dfrac{v_\mathrm{r}^2}{2}\dfrac{L'_d - L_q}{L'_d L_q}\cos 2\delta_\mathrm{r}, \\ q_\mathrm{i} \triangleq \dfrac{v_\mathrm{r}V_\infty}{L_\infty}\cos(\delta_\mathrm{r} - \delta) - \dfrac{v_\mathrm{r}^2}{L_\infty}, \end{cases} \tag{8}$$

where V_∞ denotes the infinite bus voltage, and L_∞ the inductance in the ac transmission line. In (7) the variable φ_r is defined as the power factor angle of the rectifier, and K_I is equivalent to the coupling coefficient between the ac and dc current. In (7) the first and second equations represent the relationship between the active and reactive power in the ac/dc system based on the variable φ_r. On the other hand, the third equation represents the active power relationship between the ac system and dc transmission. The averaged current relation is here assumed to derive (7) as follows:

$$i_{\mathrm{r}} \approx K_I I_{\mathrm{dc}}, \tag{9}$$

where i_{r} denotes the amplitude of the ac current at the rectifier side.

The following DAE system is hence derived for the transient stability analysis of the ac/dc power system in Fig. 1:

$$\mathsf{M}\dot{\boldsymbol{x}} = \boldsymbol{f}(\boldsymbol{x},\boldsymbol{y}), \quad \boldsymbol{0} = \boldsymbol{g}(\boldsymbol{x},\boldsymbol{y}), \tag{10}$$

where M is the positive-definite matrix:

$$\mathsf{M} \triangleq \mathsf{diag}\left(\frac{T'_{d0}}{L_d - L'_d}, 1, 2H, L_{\mathrm{dc}}\right). \tag{11}$$

In (10) $\boldsymbol{f}$ stands for the right-hand sides of (1) and (6), $\boldsymbol{g}$ the right-hand side of (7), $\boldsymbol{x}$ the vector $(v'_q, \delta, \omega, I_{\mathrm{dc}})^{\mathrm{T}} \in X$ and $\boldsymbol{y}$ the vector $(v_{\mathrm{r}}, \delta_{\mathrm{r}}, \varphi_{\mathrm{r}})^{\mathrm{T}} \in Y$. T denotes the transpose operation of vectors.

3. Summarized Theory of Differential-Algebraic Equation System

In this section we summarize fundamental concepts of the theory of the DAE system (10) based on [10]–[12].

The following two sets L and S are defined for the DAE system (10) by

$$\begin{cases} L \triangleq \{(\boldsymbol{x},\boldsymbol{y}) \in X \times Y\,;\, \boldsymbol{g}(\boldsymbol{x},\boldsymbol{y}) = \boldsymbol{0}\}, \\ S \triangleq \{(\boldsymbol{x},\boldsymbol{y}) \in L\,;\, \det(\mathrm{D}_y\boldsymbol{g})(\boldsymbol{x},\boldsymbol{y}) = 0\}, \end{cases} \tag{12}$$

where $\mathrm{D}_y\boldsymbol{g}$ stands for the Jacobian of $\boldsymbol{g}$ with respect to $\boldsymbol{y}$. Any solution in the DAE system (10) exists on L. S is called a *singular surface*, and decomposes L into several disjoint components Γ_i. If all the points on some Γ_i are such that $\mathrm{D}_y\boldsymbol{g}$ has eigenvalues with negative real parts, then Γ_i is called a *stable* component; otherwise, it is called an *unstable* component. The existence of Γ_{s} is important in order to investigate the dynamics of the DAE system (10) via singular perturbation techniques.

An EP on $L \setminus S$ is said to be *hyperbolic* if and only if the stable mapping:

$$\mathscr{M} \triangleq \mathrm{D}_x(\mathsf{M}^{-1}\boldsymbol{f}) - \mathrm{D}_y(\mathsf{M}^{-1}\boldsymbol{f})(\mathrm{D}_y\boldsymbol{g})^{-1}\mathrm{D}_x\boldsymbol{g}, \tag{13}$$

evaluated at the EP has no eigenvalues with zero real parts. The *stability region* of a stable EP $(\boldsymbol{x}_{\mathrm{s}}, \boldsymbol{y}_{\mathrm{s}})$ in a stable component Γ_{s} is defined as follows:

$$A(\boldsymbol{x}_{\mathrm{s}},\boldsymbol{y}_{\mathrm{s}}) \triangleq \{(\boldsymbol{x},\boldsymbol{y}) \in \Gamma_{\mathrm{s}};\ \lim_{t\to+\infty} \phi_t(\boldsymbol{x},\boldsymbol{y}) = (\boldsymbol{x}_{\mathrm{s}},\boldsymbol{y}_{\mathrm{s}})\}, \tag{14}$$

where $\phi_t(\cdot,\cdot)$ denotes a *flow* defined by the vector field on Γ_{s}. The boundary of $A(\boldsymbol{x}_{\mathrm{s}},\boldsymbol{y}_{\mathrm{s}})$ (in Γ_{s}) is called a *stability boundary*, denoted by $\partial A(\boldsymbol{x}_{\mathrm{s}},\boldsymbol{y}_{\mathrm{s}})$. For a hyperbolic EP $(\hat{\boldsymbol{x}},\hat{\boldsymbol{y}})$ of the DAE system (10) its *stable* and *unstable manifolds* $W^{\mathrm{s}}(\hat{\boldsymbol{x}},\hat{\boldsymbol{y}})$ and $W^{\mathrm{u}}(\hat{\boldsymbol{x}},\hat{\boldsymbol{y}})$ are defined by

$$\begin{cases} W^{\mathrm{s}}(\hat{\boldsymbol{x}},\hat{\boldsymbol{y}}) \triangleq \{(\boldsymbol{x},\boldsymbol{y}) \in \Gamma_{\mathrm{s}};\ \lim_{t\to+\infty} \phi_t(\boldsymbol{x},\boldsymbol{y}) = (\hat{\boldsymbol{x}},\hat{\boldsymbol{y}})\}, \\ W^{\mathrm{u}}(\hat{\boldsymbol{x}},\hat{\boldsymbol{y}}) \triangleq \{(\boldsymbol{x},\boldsymbol{y}) \in \Gamma_{\mathrm{s}};\ \lim_{t\to-\infty} \phi_t(\boldsymbol{x},\boldsymbol{y}) = (\hat{\boldsymbol{x}},\hat{\boldsymbol{y}})\}. \end{cases} \tag{15}$$

We say that two m-dimensional differentiable manifold M and n-dimensional differentiable manifold N intersect *transversally* if at every point $z \in M \cap N$ the sum of the tangent spaces T_zM and T_zN equals $\mathbb{R}^{m+n}$.

Lastly let us revisit the definition of energy function for the associated SP system:

$$\mathsf{M}\dot{\boldsymbol{x}} = \boldsymbol{f}(\boldsymbol{x},\boldsymbol{y}), \quad \varepsilon\dot{\boldsymbol{y}} = \boldsymbol{g}(\boldsymbol{x},\boldsymbol{y}), \tag{16}$$

where ε is small positive parameter. An energy function for the SP system (16) is defined as follows:

Definition: [11] A smooth function $\mathcal{W} : X \times Y \to \mathbb{R}$ is called an *energy function* for the SP system (16) if the following three conditions are satisfied:

(i) the derivative of $\mathcal{W}$ along any system trajectory is non-positive, i.e.

$$\dot{\mathcal{W}} = \mathrm{D}_x\mathcal{W}\mathsf{M}^{-1}\boldsymbol{f} + \frac{1}{\varepsilon}\mathrm{D}_y\mathcal{W}\boldsymbol{g} \le 0. \tag{17}$$

(ii) if $(\boldsymbol{x}(t),\boldsymbol{y}(t))$ is a non-trivial trajectory (i.e. $(\boldsymbol{x}(t),\boldsymbol{y}(t))$ is not at any EP), then along the non-trivial trajectory $(\boldsymbol{x}(t),\boldsymbol{y}(t))$ the set

$$\{t \in \mathbb{R}\,;\, \dot{\mathcal{W}}(\boldsymbol{x}(t),\boldsymbol{y}(t)) = 0\} \tag{18}$$

has measure zero in $\mathbb{R}$.

(iii) if a trajectory $(\boldsymbol{x}(t),\boldsymbol{y}(t))$ has a bounded value of $\mathcal{W}(\boldsymbol{x}(t),\boldsymbol{y}(t))$ for $t \in \mathbb{R}^+$, then the trajectory $(\boldsymbol{x}(t),\boldsymbol{y}(t))$ is also bounded.

4. Characterization of Stability Boundaries: Theoretical Result

This section discusses stability boundaries in the electric power system with dc transmission in Fig. 1. We derive an energy function for the associated SP system (16) thereby characterizing the stability boundaries.

4.1 Re-formalization of DAE System via Structure Preserving Power System Model

The DAE system (10) is rewritten via structure preserving power system model [13]. The following variables transformations are introduced:

$$\theta_{\mathrm{r}} \triangleq \delta - \delta_{\mathrm{r}}, \quad V_{\mathrm{r}} \triangleq \ln v_{\mathrm{r}}, \tag{19}$$

where we assume that $v_{\mathrm{r}} > 0$ and $\mathrm{e}^{V_{\mathrm{r}}} < K$ for some positive number K. We here define a smooth function $\mathcal{W}(v'_q, \delta, \omega, I_{\mathrm{dc}}, \theta_{\mathrm{r}}, V_{\mathrm{r}})$ by

$$\mathcal{W} \triangleq \frac{1}{2}(2H)\omega^2 + \mathcal{U}_{\mathrm{ac}}(v'_q, \delta, \omega, \theta_{\mathrm{r}}, V_{\mathrm{r}}) + \mathcal{U}_{\mathrm{dc}}(I_{\mathrm{dc}}), \tag{20}$$

where

$$\begin{cases} \mathcal{U}_{\mathrm{ac}} \triangleq -p_{\mathrm{m}}\delta \\ \quad -\dfrac{(L'_d - L_q)\cos 2(\delta-\theta_{\mathrm{r}}) - (L'_d + L_q)}{2L'_d L_q}\dfrac{\mathrm{e}^{2V_{\mathrm{r}}}}{2} \\ \quad -\dfrac{v'_q \mathrm{e}^{V_{\mathrm{r}}}}{L'_d}\cos(\delta-\theta_{\mathrm{r}}) - \dfrac{\mathrm{e}^{V_{\mathrm{r}}}V_\infty}{L_\infty}\cos\theta_{\mathrm{r}} + \dfrac{\mathrm{e}^{2V_{\mathrm{r}}}}{2L_\infty} \\ \quad -\dfrac{V_0}{L_d - L'_d}v'_q + \dfrac{L_d}{L'_d(L_d-L'_d)}\dfrac{v'^2_q}{2}, \\ \mathcal{U}_{\mathrm{dc}} \triangleq \dfrac{1}{2}R_{\mathrm{dc}}I_{\mathrm{dc}}^2. \end{cases} \tag{21}$$

The DAE system (10) is then re-formalized as follows:

$$\begin{cases} \dfrac{T'_{d0}}{L_d - L'_d}\dot{v}'_q = -\dfrac{\partial \mathcal{W}}{\partial v'_q}, \\ \dot{\delta} \qquad = \dfrac{1}{2H}\dfrac{\partial \mathcal{W}}{\partial \omega}, \\ 2H\dot{\omega} \qquad = -D\omega - \dfrac{\partial \mathcal{W}}{\partial \delta}, \\ L_{\mathrm{dc}}\dot{I}_{\mathrm{dc}} \qquad = -\dfrac{\partial \mathcal{W}}{\partial I_{\mathrm{dc}}} \\ \qquad\qquad + \mu\bar{K}_V(\mathrm{e}^{V_{\mathrm{r}}}\cos\alpha - V_{\mathrm{i}}\cos\gamma), \\ 0 \qquad = -\dfrac{\partial \mathcal{W}}{\partial \theta_{\mathrm{r}}} - \mu\bar{K}_I \mathrm{e}^{V_{\mathrm{r}}} I_{\mathrm{dc}}\cos\varphi_{\mathrm{r}}, \\ 0 \qquad = -\dfrac{\partial \mathcal{W}}{\partial V_{\mathrm{r}}} - \mu\bar{K}_I \mathrm{e}^{V_{\mathrm{r}}} I_{\mathrm{dc}}\sin\varphi_{\mathrm{r}}, \\ 0 \qquad = \mu\Big\{\bar{K}_I \mathrm{e}^{V_{\mathrm{r}}} I_{\mathrm{dc}}\cos\varphi_{\mathrm{r}} \\ \qquad\qquad - \left(\bar{K}_V \mathrm{e}^{V_{\mathrm{r}}}\cos\alpha - \dfrac{3}{\pi}\bar{X}_{\mathrm{c}}I_{\mathrm{dc}}\right)I_{\mathrm{dc}}\Big\}, \end{cases} \tag{22}$$

where $\mu \geq 0$ is the perturbation parameter: $\mu\bar{K}_V \triangleq K_V$, $\mu\bar{K}_I \triangleq K_I$ and $\mu\bar{X}_{\mathrm{c}} \triangleq X_{\mathrm{c}}$.

4.2 Characterization via Energy Function

In the section we characterize a stability boundary of a stable EP in the DAE system (10). Let ∂A and ∂A_ε be stability boundaries of the DAE system (10) and the associated SP system (16), respectively, of a stable EP $(\boldsymbol{x}_{\mathrm{s}}, \boldsymbol{y}_{\mathrm{s}})$ which lies on a stable component Γ_{s}. We now make the following assumptions for the associated SP system (16) pertinent to the characterization of the stability boundaries ∂A_ε and ∂A:

Assumptions:

(**A1**) All the EPs on ∂A_ε are hyperbolic,
(**A2**) The stable and unstable manifolds of the EPs on ∂A_ε satisfy the transversality condition,
(**A3**) The SP system possesses an energy function.

Assumptions (A1) and (A2) are generic properties for dynamical systems [14]. Assumption (A3) is therefore crucial for the application of the theorem. It is shown in Theorem 4-2 of [11] that if there exists an energy function for the associated SP system (16), then every trajectory on the stability boundary ∂A_ε converges to one of the equilibrium points on ∂A_ε as time increases. This property directly leads to the characterization of the stability boundaries ∂A_ε and ∂A.

This paper focuses on the following theorem which characterizes the stability boundary ∂A in the DAE system (10):

Theorem: [10] If Assumption (A3) is satisfied, then

$$\partial A = \partial A_\varepsilon \cap \Gamma_{\mathrm{s}}. \tag{23}$$

Suppose that further Assumptions (A1) and (A2) are satisfied. Let $(\hat{\boldsymbol{x}}_i, \hat{\boldsymbol{y}}_i)$ $i = 1, 2, \ldots$ be the EPs on the stability boundary ∂A_ε. Then

$$\partial A = \left\{ \bigcup_{(\hat{\boldsymbol{x}}_i,\hat{\boldsymbol{y}}_i)\in\partial A} W^{\mathrm{s}}(\hat{\boldsymbol{x}}_i, \hat{\boldsymbol{y}}_i) \right\} \cup \left\{ \bigcup_{(\hat{\boldsymbol{x}}_i,\hat{\boldsymbol{y}}_i)\in\partial A_\varepsilon\setminus\Gamma_{\mathrm{s}}} W^{\mathrm{s}}_\varepsilon(\hat{\boldsymbol{x}}_i, \hat{\boldsymbol{y}}_i) \cap \Gamma_{\mathrm{s}} \right\}, \tag{24}$$

where $W^{\mathrm{s}}_\varepsilon(\hat{\boldsymbol{x}}_i, \hat{\boldsymbol{y}}_i)$ stands for the stable manifold of $(\hat{\boldsymbol{x}}_i, \hat{\boldsymbol{y}}_i)$ in the associated SP system (16).

The theorem states global structure of the stability boundary as follows. ∂A consists of two parts: the first part is the set whose trajectories always converge to an EP, while the second part contains points whose trajectories reach singular surface S. In addition this theorem shows that under Assumptions (A1)–(A3) the stability boundary ∂A can be examined through the associated SP system (16). The detail structure of the second part is delineated via singular transformation [12].

4.2.1 AC Power System: $\mu = 0$

This subsection performs the characterization of the stability boundaries in the DAE system (10) under the condition $\mu = 0$. We then can discuss the dynamics of the ac system independently on that of the dc transmission; Apparently $I_{\mathrm{dc}}(t) \to 0$ as $t \to +\infty$. The setting at $\mu = 0$ therefore corresponds to the characterization with the only ac system. First we confirm that the function $\mathcal{W}(\boldsymbol{x}, \boldsymbol{y})$ is an energy function for the associated SP system at $\mu = 0$. $\varphi_{\mathrm{r}}(t)$ can be here omitted. By differentiating $\mathcal{W}$ along any the trajectory of the associated SP system (16) we have

$$\dot{\mathcal{W}} = -\frac{L_d - L'_d}{T'_{d0}}\left(\frac{\partial \mathcal{U}_{\mathrm{ac}}}{\partial v'_q}\right)^2 - D\omega^2 - \frac{1}{L_{\mathrm{dc}}}\left(\frac{\partial \mathcal{U}_{\mathrm{dc}}}{\partial I_{\mathrm{dc}}}\right)^2 - \frac{1}{\varepsilon}\left(\frac{\partial \mathcal{U}_{\mathrm{ac}}}{\partial \theta_{\mathrm{r}}}\right)^2 - \frac{1}{\varepsilon}\left(\frac{\partial \mathcal{U}_{\mathrm{ac}}}{\partial V_{\mathrm{r}}}\right)^2 \leq 0, \tag{25}$$

where $(L_d - L'_d)/T'_{d0}$ and L_{dc} are positive in practical system, and D is assumed to be positive. The condition (i) of the energy function is therefore satisfied. Suppose that there is an interval $t \in [t_1, t_2]$ such that $\dot{\mathcal{W}}(\boldsymbol{x}(t), \boldsymbol{y}(t)) = 0$. It follows from the SP system (16) and the inequality (25) that $\omega(t) = 0$, $I_{\mathrm{dc}}(t) = 0$ and $\dot{v}'_q(t) = \dot{\delta}(t) = \dot{\theta}_{\mathrm{r}}(t) = \dot{V}_{\mathrm{r}}(t) = 0$ for $t \in [t_1, t_2]$. It then follows that the associated SP system at $\mu = 0$ is at an EP. Thus the condition (ii) of the energy function also holds. In addition we can confirm by the same way as [15] that if $v_q'(t)$, $\theta_{\rm r}(t)$ and $V_{\rm r}(t)$ are bounded for every nontrivial trajectory $(\boldsymbol{x}(t), \boldsymbol{y}(t))$ with bounded function $\mathcal{W}(\cdot,\cdot)$, then $\mathcal{W}(\boldsymbol{x}(t), \boldsymbol{y}(t))$ satisfies the condition (iii). The function $\mathcal{W}(\boldsymbol{x}, \boldsymbol{y})$ is thus an energy function for the associated SP system (16) at $\mu = 0$. The above discussion can be stated in the following proposition:

Proposition 1: If $v_q'(t)$, $\theta_{\rm r}(t)$ and $V_{\rm r}(t)$ are bounded for every nontrivial trajectory $(\boldsymbol{x}(t), \boldsymbol{y}(t))$ with bounded function $\mathcal{W}(\cdot,\cdot)$, then the function $\mathcal{W}(\boldsymbol{x}, \boldsymbol{y})$ becomes an energy function for the associated SP system (16) at $\mu = 0$.

The following proposition is obtained for the characterization of the stability boundary:

Proposition 2: Suppose that the function $\mathcal{W}(\boldsymbol{x}, \boldsymbol{y})$ is an energy function for the associated SP system (16) at $\mu = 0$. If Assumptions (A1) and (A2) are satisfied for the associated SP system (16) at $\mu = 0$, then a stability boundary ∂A^0 of a stable EP $(\boldsymbol{x}_{\rm s}, \boldsymbol{y}_{\rm s})$ in some stable component $\Gamma_{\rm s}$ in the DAE system (10) is characterized by the same formula as (24).

4.2.2 AC/DC Power System: Sufficiently Small Perturbation μ

On the other hand, we can also characterize the stability boundaries in the DAE system (10) under sufficiently small perturbation μ. Suppose that the associated SP system (16) at $\mu = 0$ satisfies Assumptions (A1)–(A3). From the last equation of (10) (or (22)) we have

$$\begin{cases} \cos\varphi_{\rm r} = \dfrac{\bar{K}_V}{\bar{K}_I}\cos\alpha - \dfrac{3\bar{X}_{\rm c}}{\pi\bar{K}_I {\rm e}^{V_{\rm r}}} I_{\rm dc}, \\ \sin\varphi_{\rm r} = \sqrt{1-\cos^2\varphi_{\rm r}}, \end{cases} \tag{26}$$

where we assume that $I_{\rm dc} > 0$ and $q_{\rm g} + q_{\rm i} (= \mu\bar{K}_I {\rm e}^{V_{\rm r}} I_{\rm dc}\sin\varphi_{\rm r}) > 0$; This is relevant during transient period in the ac/dc power system in Fig. 1. Substituting (26) to (10) makes the variable $\varphi_{\rm r}$ vanished from the DAE system (10). The associated SP system (16) at $\mu \neq 0$ is then regarded as well-known perturbed dynamical system. Hence, for the robustness of hyperbolic EPs on stability boundaries [16], under sufficiently small μ, we can characterize a stability boundary ∂A^μ of a stable EP $(\boldsymbol{x}_{\rm s}^\mu, \boldsymbol{y}_{\rm s}^\mu)$ in some stable component $\Gamma_{\rm s}^\mu$ for the DAE system (10) by the same formula as (24), that is,

$$\begin{aligned} \partial A^\mu = &\left\{ \bigcup_{(\hat{\boldsymbol{x}}_i^\mu, \hat{\boldsymbol{y}}_i^\mu)\in\partial A^\mu} W^{\rm s}(\hat{\boldsymbol{x}}_i^\mu, \hat{\boldsymbol{y}}_i^\mu) \right\} \\ &\cup \left\{ \bigcup_{(\hat{\boldsymbol{x}}_i^\mu, \hat{\boldsymbol{y}}_i^\mu)\in\partial A_\varepsilon^\mu \setminus \Gamma_{\rm s}^\mu} W_\varepsilon^{\rm s}(\hat{\boldsymbol{x}}_i^\mu, \hat{\boldsymbol{y}}_i^\mu) \cap \Gamma_{\rm s}^\mu \right\}, \end{aligned} \tag{27}$$

where $(\hat{\boldsymbol{x}}_i^\mu, \hat{\boldsymbol{y}}_i^\mu)$ $i = 1, 2, \ldots$ stand for the EPs on the stability boundary $\partial A_\varepsilon^\mu$.

The above result describes concrete global structure of the stability boundary in the electric power system with dc transmission. The obtained characterization makes it possible to apply the controlling u.e.p. method [10], [11], [17], which is an effective and practical method for estimating transient stability of ac power systems, to the ac/dc power system in Fig. 1.

5. Concrete Structure of Stability Boundary: Numerical Results

This section discusses numerical results with a stability boundary in the ac/dc power system. In [7], [9] we numerically analyze a stability boundary under the parameters $D = 0$, $\mu\bar{K}_V = \mu\bar{K}_I = 1.19$ and $\mu\bar{X}_{\rm c} = 0.12$; Other parameters setting is shown in Table 1†. In this section we attempt to confirm the obtained characterization (27) via our numerical results with the stability boundary. Several numerical results in this section have been reported in [7], [9].

We note that the damping coefficient D is fixed at 0.0 in Table 1. As seen in Sect. 4 the positiveness of D is necessary to consider the existence of energy functions for the associated SP system. Although our numerical simulations are performed under $D = 0.0$ in this section, the authors confirm that our numerical results are qualitatively identical to those at $D = 0.05$.

5.1 Equilibrium Points

Table 2 shows the locations and eigenvalues of EPs in the DAE system (10). The eigenvalues at the EPs are calculated based on the stable mapping $\mathscr{M}$. In the table, a stable EP, which is called EP#1, corresponds to a post-fault steady state of the ac/dc system. A saddle EP, which is called EP#2, also exists in the DAE system (10). EP#2 annihilates with EP#1 by the fold bifurcation as the parameter $I_{\rm dc(ref)}$ decreases: related bifurcation diagram is shown in [7].

5.2 Basin Portraits around Equilibrium Points: Hyperbolic Saddle Point on Stability Boundary ∂A^μ

This section discusses a stability boundary ∂A^μ of EP#1 by basin portraits around EP#1 and EP#2. Figure 2 shows the

Table 1 Parameters setting.

L_d	1.79	L_q	1.77	L_d'	0.34
T_{d0}'	(6.3 s) × (120π s^{-1})	V_0	1.7	$p_{\rm m}$	0.5
H	(0.89 s) × (120π s^{-1})	D	0.0	L_∞	0.883
V_∞	1.0	$L_{\rm dc}$	4.2	$R_{\rm dc}$	0.014
$V_{\rm i}$	1.0	$\mu\bar{K}_V$	1.19	$\mu\bar{K}_I$	1.19
$\mu\bar{X}_{\rm c}$	0.12	G_α	30.0	$I_{\rm dc(ref)}$	1.0

†These parameters were obtained for the practical system [3], [4].

Table 2 Locations and stability of equilibrium points.

	EP#1	EP#2
v'_q	9.753214×10^{-1}	9.800746×10^{-1}
δ	4.749342×10^{-1}	4.884706×10^{-1}
ω	0.000000	0.000000
$I_{\rm dc}$	5.899123×10^{-1}	5.716954×10^{-1}
$v_{\rm r}$	9.606723×10^{-1}	9.655860×10^{-1}
$\delta_{\rm r}$	5.765143×10^{-1}	5.731841×10^{-1}
$\varphi_{\rm r}$	4.365590×10^{-1}	4.436353×10^{-1}
α	-1.511112×10^{0}	1.620139×10^{0}
$p_{\rm g}$	5.000000×10^{-1}	5.000000×10^{-1}
$p_{\rm i}$	1.103255×10^{-1}	9.252590×10^{-2}
$q_{\rm g}$	2.475875×10^{-1}	2.478743×10^{-1}
$q_{\rm i}$	3.718883×10^{-2}	3.371123×10^{-2}
$\det(\mathrm{D}_y \boldsymbol{g})$	-2.121468	-2.123402
Eigenvalues	-7.244736×10^{-4}	-7.003787×10^{-4}
	-1.580096×10^{-4}	-1.275666×10^{-4}
	$\pm j2.991998 \times 10^{-2}$	$\pm j2.980325 \times 10^{-2}$
	-3.284533	3.371143

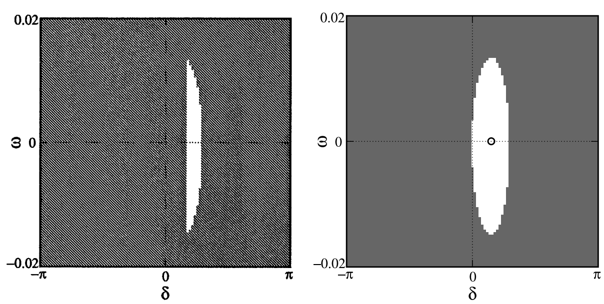

(a) $\Delta I_{\rm dc}$ = (value at EP#2)–(value at EP#1)   (b) $\Delta I_{\rm dc} = 0.0$

Fig. 2 Basin portraits around EP#1. The symbol ○ in Fig. 2(b) denotes EP#1.

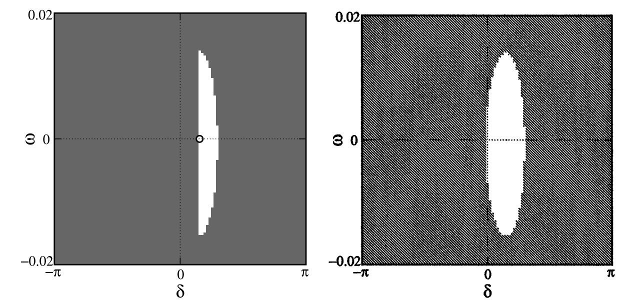

(a) $\Delta I_{\rm dc} = 0.0$ (b) $\Delta I_{\rm dc}$ = (value at EP#1)–(value at EP#2)

Fig. 3 Basin portraits around EP#2. The symbol ○ in Fig. 3(a) stands for EP#2.

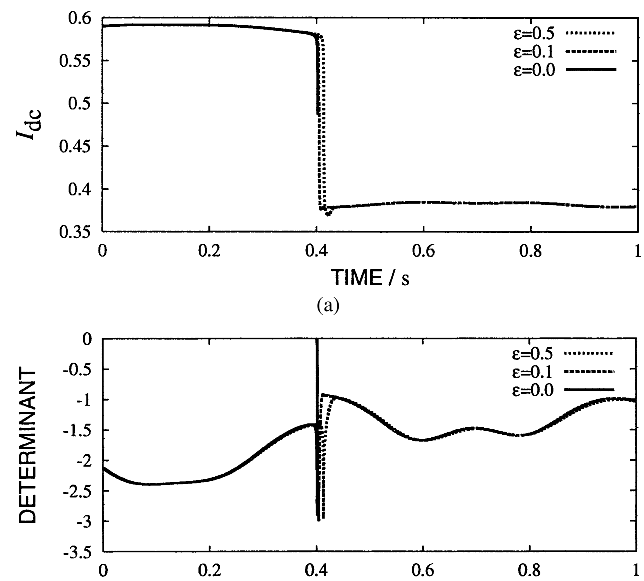

(a)

(b)

Fig. 4 Transient behavior of the DAE system (10) and associated SP system (16). All solutions in the figure start from the same initial conditions: the value of ω is 1.4×10^{-2} and other values equal those at EP#1.

basin portraits around EP#1. In the figures, initial conditions are set as follows: First v'_q is fixed at the EP's value. Second $I_{\rm dc}$ is determined as follows: $I_{\rm dc}$ = (value at EP) + $\Delta I_{\rm dc}$, where the deviation $\Delta I_{\rm dc}$ is arbitrary changed to clarify the global structure of ∂A^{μ}. Finally $(v_{\rm r}, \delta_{\rm r}, \phi_{\rm r})$ are set at the values which satisfy the algebraic constraint $\boldsymbol{g}(\boldsymbol{x}, \boldsymbol{y}) = \boldsymbol{0}$ for every initial condition (δ, ω). The numerical integration of the DAE system (10) is performed with the 3rd-stage Radau-IIA implicit Runge-Kutta method of 5th-order and 5th-stage backward differential formula [18], [19]. In Fig. 2 we adopt 101×101 cells as the initial conditions for the numerical integration. We here note that each initial condition exists in certain stable component $\Gamma_{\rm s}$ defined in Sect. 3. The initial conditions are classified in Fig. 2 as follows: the *white* region represents the basin of EP#1, and the *gray* region the one in which trajectories converge to the singular surface S. Figure 3 shows the basin portraits around EP#2. The basins are colored by the same way as in Fig. 2. This figure shows that the stable manifold of EP#2 coincides with a part of the stability boundary ∂A^{μ}; EP#2 is one of basic sets of the stability boundary ∂A^{μ}. This structure of ∂A^{μ} coincides with the first term of the obtained characterization (27). This structure and associated basic set are also clarified in [20] via straddle orbit method [21].

5.3 Straddle Orbits in Associated Singularly Perturbed System: Periodic Orbit on Stability Boundary $\partial A^{\mu}_{\varepsilon}$

Next let us consider another part of the stability boundary ∂A^{μ} shown in Figs. 2(b) and 3(a) based on the associated SP system (16). The dynamics of the SP system (16) has the similarity to that of the DAE system (10) in a stable component $\Gamma^{\mu}_{\rm s}$; This property is well-known as Tikhonov's theorem [22]. Figure 4 shows the transient behavior of the DAE system (10) and associated SP system (16). All solutions in the figure start from the same initial conditions. In Fig. 4 the solution of the DAE system converges to the singular sur-

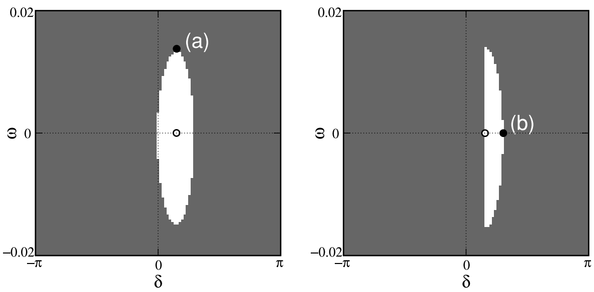

(a) Fig. 2(b) (b) Fig. 3(a)

Fig. 5 Initial conditions of straddle orbit method for the associated SP system (16).

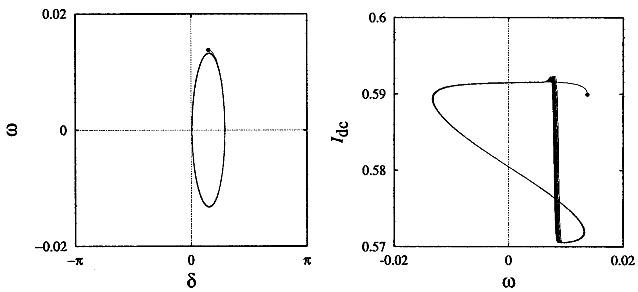

(a) From the points (a)

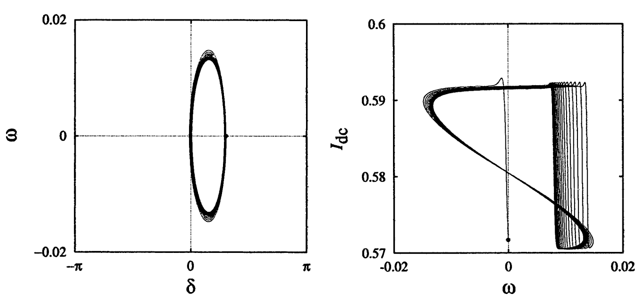

(b) From the points (b)

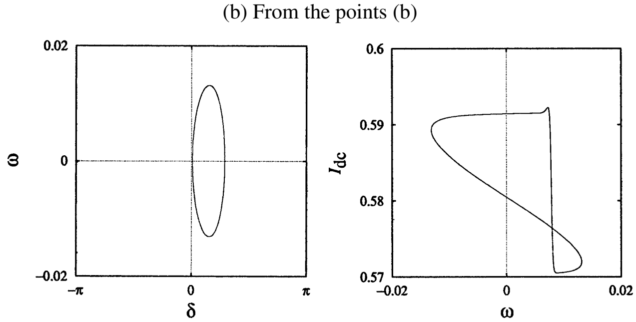

(c) Periodic orbit

Fig. 6 Projected straddle orbits and periodic orbit in the associated SP system (16) at $\varepsilon = 0.5$.

face S. On the other hand, all solutions of the associated SP system converge to another stable EP, called by EP#3. Fig. 4 implies that all solutions of the SP system show the same behavior as that of the DAE system before its solution reaches S. Thus the stability boundary ∂A^{μ} can be examined through the associated SP system (16).

We now examine basic sets related to the part of stability boundary in Figs. 2(b) and 3(a) by the straddle orbit method for the associated SP system (16). In principle any straddle orbit goes to one of basic sets whose stable manifold consists of a part of the stability boundary. Figure 5 shows the initial conditions which we fix to calculate the straddle orbits. In each condition one point exists in the basin of EP#1, another point in the basin of EP#3 for the SP system (16). Figure 6 shows the obtained straddle orbits at $\varepsilon = 0.5$ for the SP system (16). Each straddle orbit is described by being projected onto δ-ω and ω-$I_{\rm dc}$ planes. In Fig. 6 all straddle orbits converge to a periodic orbit, shown in Fig. 6(c), which is contained in the stable component $\Gamma_{\rm s}$; The periodic orbit is one of the basic sets of the stability boundary $\partial A^{\mu}_{\varepsilon}$ in the associated SP system (16). The existence shows that the obtained characterization (27) cannot be applied to the DAE system (10) under the practical parameters as discussed in the last section.

6. Summary and Discussion

This paper addressed stability boundaries analysis of the electric power system with dc transmission. The analysis was theoretically and numerically performed based on the DAE system. In Sect. 4 we completely characterized stability boundaries of the DAE system. The obtained result sheds a new insight on the stability boundaries of the ac/dc power system. In addition the characterization makes it possible to apply the controlling u.e.p. method [10], [11], [17] to the ac/dc power system in Fig. 1.

On the other hand, Sect. 5 confirmed the obtained characterization via our numerical results with the stability boundary ∂A^{μ}. It is shown that a periodic orbit exists on the stability boundary $\partial A^{\mu}_{\varepsilon}$. This implies that the phase structure of the SP system at $\mu = 0$ does not persist under the existence of the perturbation terms which represent the interaction between the ac system and dc transmission. We therefore conclude that the obtained result in Sect. 4 is inadequate to clarify the stability boundary in the DAE system under the parameters setting in Table 1.

An important question we now address is how to confirm our numerical results with the stability boundary theoretically. It is inevitable to clarify stability boundaries in the ac/dc power system shown in Fig. 1 in terms of operation and control techniques in future power supply networks. It is here stated that if a trajectory on $\partial A^{\mu}_{\varepsilon}$ of the associated SP system converges to an periodic solution as time increases, then there exists no energy function for the SP system; This fact is the contraposition of Theorem 4-2 in [11] (or see Sect. 4). Our numerical results in Sect. 5 therefore show one of the application limits of the characterization based on the present energy function. To confirm our numerical results in this paper we need to explore comprehensive energy function theory of stability boundaries in the DAE system.

Acknowledgments

The first author appreciates his fruitful suggestions of Professor Yoshisuke Ueda. Two of the authors (YS and TH) are also grateful to Professor Tsuyoshi Funaki for valuable discussions of dc transmissions.

References

[1] K.R. Padiyar, HVDC Power Transmission Systems: Technology and System Interactions, Wiley Eastern, New Delhi, 1990.
[2] T. Machida, ed., DC Transmission Engineering, Tokyo Denki University Press, Tokyo, 1999.
[3] Y. Sekine, S. Kato, T. Motoki, and S. Ito, "Kii channel HVdc link between Shikoku and Kansai Electric Power Companies by submarine cables," Proc. CIGRE Tokyo Symposium, no.220-04, Tokyo, Japan, 1995.
[4] T. Fujiwara, K. Matsuno, Y. Inoue, and T. Hayashi, "Study of power modulation and fast margin angle control in Kii channel HVdc link," Proc. CIGRE Tokyo Symposium, no.410-05, Tokyo, Japan, 1995.
[5] M.A. Pai, K.R. Padiyar, and C. Redhakrishna, "Transient stability analysis of multi-machine AC/DC power systems via energy-function method," IEEE Trans. Power Appar. Syst., vol.PAS-100, no.12, pp.5027–5035, 1981.
[6] Y. Susuki and T. Hikihara, "Swing phenomena and global structures of solution space in an electric power system with DC transmission," Proc. Nonlinear Dynamics of Electronic Systems, pp.133–136, Delft, The Netherlands, 2001.
[7] Y. Susuki and T. Hikihara, "An analysis with differential-algebraic equation in electric power system with DC transmission," Proc. IEEE/PES Transmission and Distribution Conference, and Exhibition 2002: Asia Pacific, vol.3, pp.1933–1936, Yokohama, Japan, 2002.
[8] C.A. Cañizares, F.L. Alvarado, C.L. DeMarco, I. Dobson, and W.F. Long, "Point of collapse methods applied to AC/DC power systems," IEEE Trans. Power Syst., vol.7, no.2, pp.673–683, 1992.
[9] Y. Susuki and T. Hikihara, "Stability region in electric power system with DC transmission based on differential-algebraic equation," Proc. Universities Power Engineering Conference, vol.2, pp.745–749, Stafford, UK, 2002.
[10] H.-D. Chiang and L. Fekih-Ahmed, "On the direct method for transient stability analysis of power system structure preserving models," Proc. Int. Symp. Circuits Syst. (ISCAS), pp.2545–2548, 1992.
[11] H.-D. Chiang, C.-C. Chu, and G. Cauley, "Direct stability analysis of electric power systems using energy functions: Theory, applications, and perspective," Proc. IEEE, vol.83, no.11, pp.1497–1529, 1995.
[12] V. Venkatasubramanian, H. Schättler, and J. Zaborszky, "Dynamics of large constrained nonlinear systems—A taxonomy theory," Proc. IEEE, vol.83, no.11, pp.1530–1561, 1995.
[13] N.A. Tsolas, A. Arapostathis, and P.P. Varaiya, "A structure preserving energy function for power system transient stability analysis," IEEE Trans. Circuits Syst., vol.CAS-32, no.10, pp.1041–1049, 1985.
[14] H.-D. Chiang, M.W. Hirsch, and F.F. Wu, "Stability regions of nonlinear autonomous dynamical systems," IEEE Trans. Autom. Control, vol.33, no.1, pp.16–27, 1988.
[15] C.-C. Chu and H.-D. Chiang, "Constructing analytical energy functions for lossless network-reduction power system models: Framework and new developments," Circuits Syst. Signal. Process., vol.18, no.1, pp.1–16, 1999.
[16] H.-D. Chiang and C.-C. Chu, "Theoretical foundation of the BCU method for direct stability analysis of network-reduction power system models with small transfer conductances," IEEE Trans. Circuits Syst. I, Fundam. Theory Appl., vol.42, no.5, pp.252–265, 1995.
[17] Y. Zou, M.-H. Yin, and H.-D. Chiang, "Theoretical foundation of the controlling UEP method for direct transient-stability analysis of network-preserving power system models," IEEE Trans. Circuits Syst. I, Fundam. Theory Appl., vol.50, no.10, pp.1324–1336, 2003.
[18] K.E. Brenan, S.L. Campbell, and L.R. Petzold, Numerical Solution of Initial-Value Problems in Differential-Algebraic Equations, North-Holland, Amsterdam, 1989.
[19] E. Hairer and G. Wanner, Solving Ordinary Differential Equations-II: Stiff and Differential-Algebraic Problems, Second Revised Edition, Springer-Verlag, New York, 1996.
[20] Y. Susuki and T. Hikihara, "Transient waveforms related to stability boundary in electric power system with DC transmission based on differential-algebraic equation," Proc. IEE Japan Annual Conference, vol.6, p.23, 2002.
[21] P.M. Battelino, C. Grebogi, E. Ott, and J.A. Yorke, "Multiple coexisting attractors, basin boundaries and basic sets," Physica D, vol.32, pp.296–305, 1988.
[22] H.K. Khalil, Nonlinear Systems, Third Edition, Prentice-Hall, New Jersey, 2002.

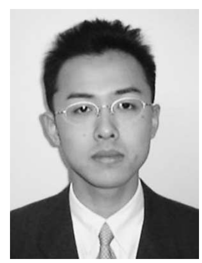

Yoshihiko Susuki was born in Hyogo, Japan on December 31, 1977. He received his bachelor and master degrees in engineering from Kyoto University in 2000 and 2002, respectively. He is currently a Ph.D. candidate in the Department of Electrical Engineering at Kyoto University. In 2003 he was a visiting scholar in the School of Electrical Engineering at Cornell University. His research interests include nonlinear dynamics, power system engineering and control applications. He is a student member of IEEE, IEEJ and ISCIE.

Takashi Hikihara received his doctoral degree in engineering from Kyoto University in 1990. In 1987 he joined the faculty of the School of Electrical Engineering at Kansai University. Since 1997 he has been with the Department of Electrical Engineering at Kyoto University, where he is currently a Professor. His research interests include experimental studies on flux-linkage dynamics in synchronous generators, development of magnetic levitation systems and HTSC bearing systems, time-delayed feedback control of chaos, synthesis and analysis of power electronics circuits, nonlinear dynamics, power engineering and so forth. He is a regular member of IEEE, IEE, IEEJ, ISCIE, SICE and APS.

Hsiao-Dong Chiang received his Ph.D. degree in electrical engineering and computer sciences from the University of California at Berkeley in 1986. After receiving the Ph.D. degree he worked on a special project at the Pacific Gas and Electricity Company, San Francisco, CA. In 1987 he joined the faculty of the School of Electrical Engineering at Cornell University, where he is currently a Professor. His current research interests are in nonlinear systems theory, computation, and application to electric circuits, signals and systems; power system stability and control, security assessments and enhancements; distribution system analysis, control and design; intelligent information processing system; drawing digitization and automated mapping/facility management; and global optimization techniques and applications.